A MULTISCALE METHOD FOR WEAKLY COUPLED OSCILLATORS

GIL ARIEL, BJORN ENGQUIST, AND RICHARD TSAI

ABSTRACT. A multiscale method for computing the effective slow behavior of a system of weakly coupled general oscillators is presented. The oscillators may be either in the form of a periodic solution or a stable limit cycle. Furthermore, the oscillators may be in resonance with one another and thereby generate some hidden slow dynamics. The proposed method relies on correctly tracking a set of slow variables that is sufficient to approximate any variable and functional that are slow under the dynamics of the ODE. The advantages of the method is demonstrated with examples. Particular emphasis is given to the effect of synchronization. Harmonic oscillators with slowly varying properties are also studied. The algorithm follows the framework of the heterogeneous multiscale method.

1. INTRODUCTION

Ordinary differential equations (ODEs) with highly oscillatory periodic solutions have been proven to be a challenging field of research from both analytic and numerical points of view [6, 7]. One typical example is the extensively studied equation of Van der Pol, known as the Van der Pol oscillator [14],

$$\ddot{x} = -x + \nu(1 - x^2)\dot{x}. \tag{1.1}$$

Equation (1.1) has a unique, stable limit cycle that tends to the circle $x^2 + \dot{x}^2 = 2$ in the limit $\nu \to 0$. A second type of oscillators arise when a system of ODEs has a family of periodic solutions. We refer to a pair (x, y), with $x, y \in \mathbb{R}^d$ as an oscillator if the trajectory $(x(t), y(t))$ is either periodic or approaches a stable periodic limit cycle. The period in both cases is denoted T_0.

In this paper we suggest an integration scheme for systems in which different oscillators are weakly coupled. The coupling strength is taken to be proportional to a small parameters $\epsilon \ll 1$. Accordingly, we are interested in the long time behavior of the dynamics, usually in the interval $0 \le t \le \epsilon^{-1}T$. Let $\{(x_i, y_i)\}_{i=1}^k$ denote a set of k oscillators with $x_i, y_i \in \mathbb{R}^{d_i}$. We consider ODE systems of the form

$$\dot{x} = f(\mathbf{x}, \mathbf{y}) + \epsilon g(\mathbf{x}),\ \mathbf{x}(0) = \mathbf{x}_0, \tag{1.2}$$

where $0 < \epsilon \ll 1$ is a small parameter that characterizes the separation of time scales in the dynamics and $\mathbf{x} = (x_1, y_1, x_2, y_2, \ldots, x_k, y_k)$. On a time scale that is independent of ϵ the term $\epsilon g(\mathbf{x})$ constitutes a small perturbation to the leading order term $f(\mathbf{x})$ and can be neglected in the limit as $\epsilon \to 0$. However, in the longer time scale of order ϵ^{-1}, this perturbation may accumulate to an important contribution that cannot be ignored. We assume that the solution of (1.2) remains in a bounded

domain $\mathcal{D}_0 \subset \mathbb{R}^d$ for $0 \leq t \leq \epsilon^{-1}T$. Here the diameter of $\mathcal{D}_0$ and $T < \infty$ are two constants independent of ϵ. Here, $T < \infty$ is a constant that is independent of ϵ. For any fixed ϵ and initial condition $\mathbf{x}(0) = \mathbf{x}_0$ we denote the solution of (1.2) by $\mathbf{x}(t; \epsilon, \mathbf{x}_0)$. For brevity we will write $\mathbf{x}(t)$ whenever it is clear what the value for ϵ and the initial conditions are.

One of the main difficulties in numerical integration of (1.2) using explicit methods, is that stability requirements force a step size that is of order one. This generally implies that the computational complexity for integrating (1.2) over a time $\epsilon^{-1}T$ is at least of the order of ϵ^{-1}. Our scheme can be applied to problems for which specialized algorithms such as the exponential integrators [8, 9] do not apply, or do not yield efficient approximations. The new schemes proposed in this manuscript generalize those in [1] to systems of nonlinear oscillators. Our method is sublinear in the frequency of the oscillators.

The various types of oscillators make a general theory difficult. As a recourse, we first describe the main idea behind our algorithm and then apply it to several examples involving different types of oscillators. The general approach is to identify a set of functions of $\mathbf{x}$ that are slow with respect to the dynamics of (1.2), i.e., along the trajectories of (1.2) the time derivatives of these functions are bounded above by $C_0\epsilon$. We classify these functions as the amplitudes and the phase differences (relative phases) of the oscillators, and we generally refer to them as slow variables of the system. System (1.2) is then integrated using the the framework of the heterogeneous multiscale method (HMM) [3, 4, 5] — a micro-solver integrates the full ODE (1.2) at different times, and each time for short time segments. With the help of the slow variables, the microscale integrations uncover the system's effective dynamics at different times. The system is then integrated very efficiently by a Macro-solver using this effective dynamics.

For convenience, Section 2 describes briefly the main results and algorithm proposed in [1]. We refer the readers to [1] for more details and an analysis of the algorithm related to accuracy, efficiency, and convergence. Section 3 analyses the slow variables admitted by ODE systems of the form of (1.2) and section 4 gives a few numerical examples. These examples are chosen in order to stress the importance of correctly tracking the relative phase between oscillators. In Section 5 we analyze a similar setup for a class of time dependent harmonic oscillators. We conclude in Section 6.

2. THE HMM SCHEME

In order to study the long time properties of (1.2) it is important to distinguish between the fast and slow constituents of the dynamics. We say that a real valued smooth function (variable) $\alpha(\mathbf{x})$ is slow with respect to (1.2) if there exists a non

empty open set $\mathcal{A} \subset \mathbb{R}^d$ such that

$$\max_{\mathbf{x}_0 \in \mathcal{A}, t \in \mathcal{I}} \left| \frac{d}{dt} \alpha(\mathbf{x}(t; \epsilon, \mathbf{x}_0)) \right| \leq C_0 \epsilon \tag{2.1}$$

where C_0 is a constant that is independent of ϵ and $\mathcal{I} = [0, \epsilon^{-1}T]$. Otherwise, $\alpha(\mathbf{x})$ is said to be fast. Similarly, we say that a quantity or constant is of order one if it is bounded independent of ϵ.

In [1] we suggested looking for a set of slow variables $\xi = (\xi_1(\mathbf{x}), \ldots, \xi_r(\mathbf{x}))$ that is sufficient to approximate any smooth variable or functional that is slow under the dynamics of the ODE. In other words, any variable $\alpha(\mathbf{x})$ that is slow with respect to (1.2) can be written as $\alpha(\mathbf{x}) = \tilde{\alpha}(\xi(\mathbf{x}))$ for some function $\tilde{\alpha} : \mathbb{R}^r \to \mathbb{R}^d$. The functions $\xi_1(\mathbf{x}), \ldots, \xi_r(\mathbf{x})$ are functionally independent, i.e., $\nabla\xi_1(\mathbf{x}), \ldots, \nabla\xi_r(\mathbf{x})$ are linearly independent in the open set $\mathcal{A}$. Augmenting the slow variables with $d-r$ fast ones $z = (z_1, \ldots, x_{d-r})$ such that $\partial(\xi, z)/\partial\mathbf{x} \neq 0$ in $\mathcal{A}$, the new coordinate system can be thought of as a chart. We will refer to such a chart that has a maximal number of slow variables as a maximally slow chart (or a slow chart for shorthand) in $\mathcal{A}$ with respect to the dynamics (1.2). Covering the set $\mathcal{D}_0$ by maximally slow charts we obtain an maximally slow atlas for $\mathcal{D}_0$. Consequently, averaging theory [12] implies that for small ϵ, $\xi(\mathbf{x}(t; \epsilon, \mathbf{x}_0))$, is well approximated in $\mathcal{I}$ by an effective equation of the form

$$\dot{\xi} = \epsilon F(\xi),\ \xi(0) = \xi(\mathbf{x}_0). \tag{2.2}$$

This statement in proven in [1]. We do not assume that the effective equation (2.2) is available as an explicit formula. Instead, the idea behind the HMM algorithm is to evaluate $F(\xi)$ by numerical solutions of the original ODE (1.2) on significantly reduced time intervals. In this way, the HMM algorithm approximates an assumed effective equation whose form is typically unknown. This strategy is advantageous if one can approximate $F(\xi)$ efficiently.

A key step in applying the algorithm is the identification of a slow atlas. In a section of [1], we present both analytic and numerical methods for finding such an atlas for the simple case in which $f(\mathbf{x})$ is linear, i.e., $f(\mathbf{x}) = A\mathbf{x}$ where A is a diagonalizable matrix whose eigenvalues have non-positive real parts. It is then proven that the slow atlas for the ODE can be described using a single chart which consists of the following slow variables:

- Trivial slow variables that correspond to a basis for the Null space of A.
- Amplitudes of oscillators (or rather square of), which are quadratic functions of $\mathbf{x}$.
- The relative phase between pairs of oscillators which correspond to some specific coupling of different oscillators through initial conditions. If the ratio between the frequencies of two oscillators is a rational number, then this relative phase can be expressed as a polynomial in $\mathbf{x}$.

A simple example is the following system described by

$$\begin{pmatrix} 0 & 1 & 0 & 0 & 0 \\ -1 & 0 & 0 & 0 & 0 \\ 0 & 0 & 0 & 1 & 0 \\ 0 & 0 & -1 & 0 & 0 \\ 0 & 0 & 0 & 0 & 0 \end{pmatrix}. \tag{2.3}$$

Here (x_1, x_2) and (x_3, x_4) are harmonic oscillators with frequency $1/2\pi$. It is easily verified that the amplitudes $I_1 = x_1^2 + x_2^2$ and $I_1 = x_2^2 + x_4^2$ and the relative phase $J_1 = x_1 x_3 + y_x + 2x + 4$ are slow variables. In addition, x_5 is trivially slow.

The main purpose of this paper is to extend these ideas to a wider class of ODEs. We find that the slow charts have the same structure, i.e., it consists of generalized concepts of amplitudes and relative phases. A few typical examples for which this program can be carried through are analyzed in the following sections.

2.1. **The algorithm.** Suppose $\xi = (\xi_1(\mathbf{x}), \ldots, \xi_r(\mathbf{x}))$ is a slow atlas for (1.2). The ODE (1.2) is integrated using a two level algorithm. Each level corresponds to the integration of (1.2) on a different time scale. The first is a Macro-solver, which integrates an effective equation for the slow variables ξ (2.2). The second level is a micro-solver that is invoked whenever the Macro-solver needs an estimation of the effective equation. Each time the micro-solver is invoked, it computes a short time solution of (1.2) using a suitable initial data. The time derivative of ξ is approximated by

$$\dot{\xi}(t) \sim \langle \dot{\xi}(t) \rangle_\eta = \int_0^\eta \dot{\xi}(t+\tau) K_\eta(t+\eta-\tau) d\tau, \tag{2.4}$$

where, $K(\cdot)$ denotes a smooth averaging kernel. Note that $\dot{\xi}$ is not necessarily slow, but is bounded independent of ϵ. The properties of averaging with respect to a kernel will be discussed shortly. Sample times of the Macro-solver are denoted $t_0, \ldots, t_N$, where $N = \epsilon^{-1} T/H$. The output of the Macro-solver is denoted $\mathbf{x}_0, \ldots, \mathbf{x}_N$. The output of the micro-solver with step size h, initiated at time t_n with initial conditions $\mathbf{x}_n$ is denoted $\mathbf{x}_n^1, \ldots, \mathbf{x}_n^M$, where $M = \eta/h$ is taken to be an even integer. The structure of the algorithm, depicted in Figure 1, is as follows.

(1) Initial conditions: $\mathbf{x}(0) = \mathbf{x}_0$ and $n = 0$.
(2) Force estimation:
   (a) micro-simulation: Solve (1.2) in $[t_n, t_n + \eta]$ with initial conditions $\mathbf{x}(t_n) = \mathbf{x}_n$.
   (b) averaging: approximate $\dot{\xi}(t_n)$ by $\langle \dot{\xi}(t_n) \rangle_\eta$.
(3) Macro-step (exemplified by Forward Euler scheme):
   $\mathbf{x}_{n+1} = \mathbf{x}_{\text{mid}} + H\delta\mathbf{x}$, where $\mathbf{x}_{\text{mid}} = \mathbf{x}_n^{M/2}$ is the position at the middle of the micro simulation and $\delta\mathbf{x}$ is the least squares solution of the linear system

$$\delta\mathbf{x} \cdot \nabla \xi_i(\mathbf{x}_{\text{mid}}) = F_i(\xi(\mathbf{x}_{\text{mid}})) = \langle \dot{\xi}_i \rangle_\eta,$$

for all $i = 1 \dots r$.

(4) $n = n + 1$. Repeat steps (2) and (3) to time $\epsilon^{-1}T$.

The averaged time derivative of ξ, $\langle \dot{\xi} \rangle_\eta = \dot{\xi} * K_\eta$, can be calculated using either the chain rule as $\dot{\xi} = \nabla \xi \cdot \dot{x} = \nabla \xi \cdot (f(\mathbf{x}) + \epsilon g(\mathbf{x}))$, or using integration by parts as $\dot{\xi} * K_\eta = -\xi * K'_\eta$.

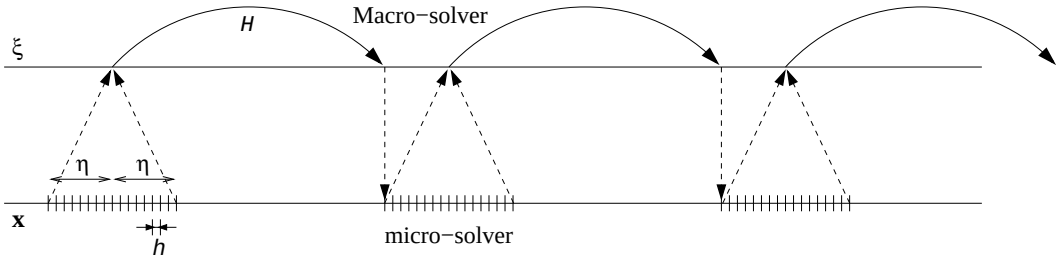

FIGURE 1. The cartoon depicts the time steps taken by the HMM scheme. At the n-th macro step, a micro-solver with step size h integrates (1.2) to approximate $\mathbf{x}(t)$ in a time segment $[t_n, t_n + \eta]$. This data is used to calculate $\langle \xi(\mathbf{x}(t)) \rangle_\eta$. Then, the Macro-solver takes a big step of size $H\delta\mathbf{x}$, where $\delta\mathbf{x}$ is consistent with $\langle \dot{\xi} \rangle_\eta$, i.e., $\delta\mathbf{x} \cdot \nabla \xi_i = \langle \dot{\xi}_i \rangle_\eta$ for all identified slow variables ξ_i.

Let $K(\cdot)$ denote a smooth kernel function with support on $[0, 1]$ such that $\int_0^1 K(\tau)d\tau = 1$ and $\int_0^1 K(\tau)(\tau - 1/2)d\tau = 0$. For simplicity, we assume that $K(\cdot)$ is symmetric with respect to its mid point. Also, for $\eta > 0$ let

$$K_\eta(\cdot) = \eta^{-1} K(\eta^{-1} \cdot). \tag{2.5}$$

We will take η to be ϵ dependent such that $0 < \eta \ll \epsilon^{-1}$. The convolution of a function $a(t)$ with K_η is denoted as

$$\langle a(t) \rangle_\eta = (a * K_\eta)(t) = \int_0^\eta a(\tau) K_\eta(t - \tau) d\tau. \tag{2.6}$$

Typically, the fast dynamics in equations such as (1.2) is one of two types (compare to the linear case $f = A\mathbf{x}$). The first consists of modes that are attracted to a low dimensional manifold in a time scale of order one. These modes are referred to as transient or dissipative modes. The second type consists of oscillators with constant or slowly changing frequencies that are independent of ϵ. For sufficiently large values of $\eta = \eta(\epsilon)$, averaging with respect to the kernel approximates the asymptotic dynamics of the different modes. With a symmetric kernel, dissipative variables are practically relaxed and negligible at the midpoint of the time interval in integral (2.6). Averaging of oscillatory modes filters out high frequency oscillations and approximates the slow parts of the dynamics. The errors introduced by the averaging is estimated in [1]. Asymmetric kernels can also be used in order to obtain an improved accuracy.

3. SLOW VARIABLES

Let (x, y) denote an oscillator. First, we would like to generalize the concepts of amplitude and phase of harmonic oscillators to non-harmonic ones. This will allow us to identify the slow variables in the weak coupling case (1.2). For simplicity, we consider 1-dimensional oscillators, i.e., $x, y \in \mathbb{R}$. Higher dimensions can be treated similarly.

3.1. **Uncoupled oscillators.** We consider several examples.

Harmonic oscillator: Consider the simple linear ODE

$$\begin{cases} \dot{x} &= \omega y \\ \dot{y} &= -\omega x, \end{cases} \tag{3.1}$$

where $\omega \in \mathbb{R}$. The amplitude of the oscillator is given by $I_{\rm har} = x^2 + y^2$. It is a slow variable since $\dot{I}_{\rm har} = 0$. The phase ϕ is given by $\tan \phi_{\rm har} = x/y$. Hence, $\dot{\phi}_{\rm har} = 1$.

Van der Pol oscillator: Consider (1.1) with $\nu = \epsilon$:

$$\begin{cases} \dot{x} &= y \\ \dot{y} &= -x + \epsilon(1 - x^2)y. \end{cases} \tag{3.2}$$

To leading order in ϵ, this example is the same as the harmonic one. Hence, one can still take the amplitude as $I_{\rm vdp} = x^2 + y^2$. It is a slow variable since $\dot{I}_{\rm vdp} = 2\epsilon(1 - x^2)y^2 = O(\epsilon)$. The phase $\phi_{\rm vdp}$ is given by $\tan \phi_{\rm vdp} = x/y$ and $\dot{\phi}_{\rm vdp} = 1 + \epsilon(1 - x^2)y/I_{\rm vdp}$.

Volterra-Lotka oscillator: A version of the Volterra-Lotka oscillator takes the form

$$\begin{cases} \dot{x} &= x(1 - y) \\ \dot{y} &= \nu^{-1} y(x - 1), \end{cases} \tag{3.3}$$

where $\nu > 0$ satisfies $\epsilon \ll \nu \ll 1$. Equation (3.3) admits a family of periodic solutions that can be parametrized according to the initial conditions $0 < x(0) < 1$ and $y(0) = 1$. An example trajectory is depicted in Figure 2. The trajectory along a single period can be divided into two parts. The first is a relatively slow movement close to the $y = 0$ line. The second segment is a rapid relaxation along the upper arc depicted in Figure 2. The relaxation time is of the order of ν. It can be verified that $I_{\rm vl} = x - \ln x + \nu(y - \ln y)$ is a constant of motion; i.e., $\dot{I}_{\rm vl} = 0$. Hence, it may serve as an amplitude of the oscillator.

In order to get a notion of phase, as in [11], we parametrize a single period of $(x(t), y(t))$ by time t . For small values of ν, y is a dissipative variable that relaxes to zero rapidly on a time scale of the order of ν. Hence, we can use the variable x to track the progress along the trajectory of the oscillator and neglect the fast relaxation time, thus creating a notion of periodically changing phase. Consider the branch given by $y = 0$ and let $(x, y) = (\psi_{\rm vl}(t), \tilde{\psi}_{\rm vl}(t))$ denote a solution of (3.3)

with initial conditions at the beginning of the branch. We define the phase $\phi_{\rm vl}$ as $\phi_{\rm vl} = \psi_{\rm vl}^{-1}(x(t))$, where $\psi_{\rm vl}^{-1}$ denotes the inverse function of $\psi_{\rm vl}$. Differentiating with respect to time yields $\frac{d}{dt}\phi_{\rm vl}(\mathbf{x}(t)) = 1$.

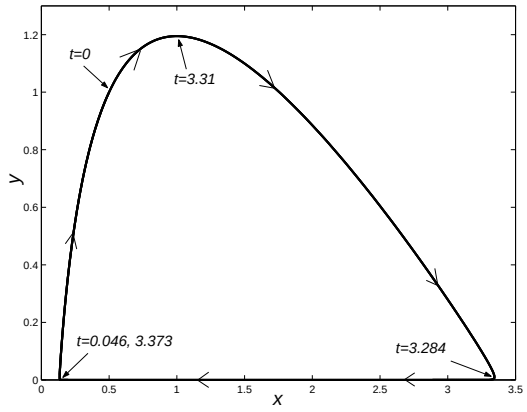

FIGURE 2. The trajectory of the Volterra-Lotka oscillator (3.3) with $\nu = 0.01$, $x(0) = 0.5$ and $y(0) = 1$.

Relaxation oscillators: Consider the following ODE used in [2]

$$\begin{cases} \dot{x} &= -1 - x + 8y^3 \\ \dot{y} &= \epsilon^{-1}(-x + y - y^3). \end{cases} \tag{3.4}$$

The dynamics of (3.4) has a slow manifold $-x + y - y^3 = 0$, depicted in Figure 3. Hence, after a short initial relaxation time of order ϵ the oscillator is attracted to a periodic limit cycle. The upper and lower branches of this cubic polynomial are stable up to the turning points at which $dx/dy = 0$. For any initial condition, the solution of $(x(t), y(t))$ is rapidly attracted to one of the stable branches on an $O(\epsilon)$ time scale. The trajectory then moves closely along the branch until it becomes unstable. At this point the solution is quickly attracted to the other stable branch. The trajectory of the oscillator is depicted in Figure 3. Van der Pol named these types of oscillators as relaxation oscillators due to the fast relaxation process at the instabilities.

In this example, the amplitude of the oscillator can be understood as the distance of the trajectory $(x(t), y(t))$ from the limit cycle. In the relaxation oscillator (3.4) this distance converges to zero exponentially fast in a time scale of order ϵ. Hence, the amplitude of the oscillator can be considered a dissipative variable.

The phase of the oscillator, $\phi_{\rm rlx}(t)$ is obtained by parameterizing the limit cycle with respect to time [11]. Note that the period, T_0, is bounded independent of ϵ. We define the phase locally on each branch of the slow manifold. The fast transitions between the stable branches are neglected since the transition time is of the order of ϵ. Without loss of generality we consider the upper branch. Let $(x(t), y(t)) = (\psi_{\rm rlx}(t), \tilde{\psi}_{\rm rlx}(t))$ denote the trajectory of (3.4) over the upper branch. Since $x(t)$ is

monotonic, we can use it to parametrize the advancement of the trajectory along the stable branch of $x = y - y^3$. Hence, we take $\phi_{\rm rlx} = \psi_{\rm rlx}^{-1}(x(t))$, where $\psi_{\rm rlx}^{-1} :\to \mathbf{t}$ denotes the inverse function of $\psi_{\rm rlx}$. As before, we have that $\dot{\phi}_{\rm rlx} = 1$. The inverse of $\psi_{\rm rlx}$ is generally hard to find. However, the numerical algorithm described in the following section only requires its derivative which is conveniently given by $(\psi_{\rm rlx}^{-1})' = 1/\psi'_{\rm rlx}$.

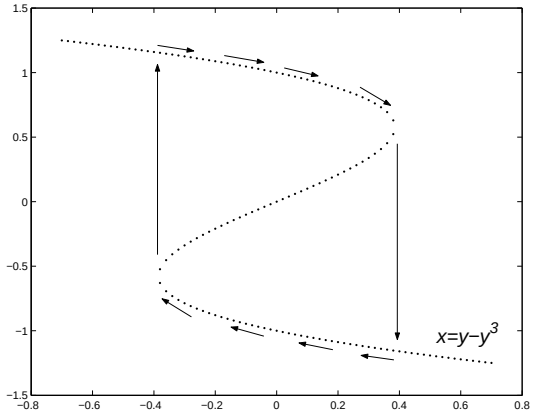

FIGURE 3. The trajectory of the relaxation oscillator (3.4).

3.2. **Coupled oscillators.** Let $\{(x_i, y_i)\}_{i=1}^k$ denote a collection oscillators. The amplitude and phase of the i'th oscillator are denoted $I_i(x_i, y_i)$ and $\phi_i(x_i, y_i)$, respectively. The solution of the coupled system (1.2) is denoted $\mathbf{x}(t) = (x_1(t), y_1(y), \ldots, x_k(t), y_k(y))$, while the solution of the decoupled system, obtained in the limit $\epsilon \to 0$, is denoted $\mathbf{x}(t) = (X_1(t), Y_1(y), \ldots, X_k(t), Y_k(y))$. The discussion on uncoupled oscillators suggests the following properties for coupled systems.

- If $I_i(X_i, Y_i)$ is slow with respect to the decoupled dynamics, then $I_i(x_i, y_i)$ is slow with respect to coupled system (1.2).
- If the variable $I_i(X_i, Y_i)$ is dissipative under the decoupled dynamics, then $I_i(x_i, y_i)$ is dissipative under the dynamics of (1.2).
- The variable $\phi_1(x_1, y_1)$ is fast.
- For all $i = 1, \ldots, k-1$, The variables $J_i = \phi_{i+1}(x_{i+1}, y_{i+1}) - \phi_i(x_i, y_i)$ are slow with respect to (1.2).

The set of variables $\tilde{\mathbf{x}} = (I_1, \ldots, I_k, \phi_1, J_1, \ldots, J_{k-1})$ decomposes the dynamics of the system into slow variables (slow amplitudes and relative phases), dissipative ones (dissipative amplitudes), and a single periodic fast variable, ϕ_1. Furthermore, the Jacobian $\det(\partial\tilde{\mathbf{x}}/\partial\mathbf{x}) \neq 0$, i.e., $\tilde{\mathbf{x}}$ is a change of variables. Let $\xi = (\xi_1, \ldots, \xi_r)$ denote a vector consisting of only the slow coordinates of $\tilde{\mathbf{x}}$. By a dimensionality count we see that ξ is a maximally slow chart for (1.2). Since the relative phase is defined locally on particular stable branches of the dynamics, the chart is also

defined locally. The slow atlas is obtained by patching different charts into a global coordinate system that consists of the slow variables in each localized region.

As an example, let us consider a relaxation oscillator (3.4), coupled to a harmonic one (3.1):

$$\begin{cases} \dot{x}_1 &= \omega y_1 + \epsilon g_1(\mathbf{x}) \\ \dot{y}_1 &= -\omega x_1(\mathbf{x}) \\ \dot{x}_2 &= -1 - x_2 + 8y^3 + \epsilon g_2(\mathbf{x}) \\ \dot{y}_2 &= \epsilon^{-1}(-x + y - y^3), \end{cases} \tag{3.5}$$

A slow chart for (3.5) can be taken to be $\xi = (I_1, J_1)$, where

$$\begin{aligned} I_1 &= I_{\mathrm{har}}(x_1, y_1) = x_1^2 + y_1^2 \\ J_1 &= \phi_{\mathrm{har}}(x_2, y_2) - \phi_{\mathrm{rlx}}(x_2, y_2). \end{aligned} \tag{3.6}$$

Recall however that the amplitude of the relaxation oscillator is not a slow variable since the trajectory of the oscillator converges to a limit cycle on a time scale that is of the order of ϵ.

The algorithm described in Section 2.1 requires solving an under-determined system at every Macro step in order to find a displacement $\delta\mathbf{x}$ that is consistent with the macroscopic evolution of the slow variables. For the example at hand this system reads

$$\begin{aligned} \delta\mathbf{x} \cdot \nabla I_1(\mathbf{x}_{\mathrm{mid}}) &= \langle \dot{I}_1 \rangle_\eta = \langle \frac{d}{dt} I_1(\mathbf{x}(\cdot)) \rangle_\eta \\ \delta\mathbf{x} \cdot \nabla (J_1)(\mathbf{x}_{\mathrm{mid}}) &= \langle \dot{J}_1 \rangle_\eta = \langle \frac{d}{dt} J_1(\mathbf{x}(\cdot)) \rangle_\eta \end{aligned} \tag{3.7}$$

Recall that $\mathbf{x}_{\mathrm{mid}}$ is the position at the middle of each micro simulation. ∇J_1 is evaluated by

$$\begin{aligned} \nabla(J_1) &= \nabla\phi_{\mathrm{rlx}}(x_2, y_2) - \nabla\phi_{\mathrm{har}}(x_1, y_1) = \nabla\psi_{\mathrm{rlx}}^{-1}(x_2) - \nabla\psi_{\mathrm{har}}^{-1}(x_1) \\ &= \begin{pmatrix} -1/\psi'_{\mathrm{har}}(t(x_1)) \\ 0 \\ 1/\psi'_{\mathrm{rlx}}(t(x_2)) \\ 0 \end{pmatrix} = \begin{pmatrix} -1/(\omega y_1) \\ 0 \\ 1/(-1 - x_2 - 8y_2^3) \\ 0 \end{pmatrix}, \end{aligned} \tag{3.8}$$

for $\psi' \neq 0$. Here, being consistent with our previous definitions, $\psi_{\mathrm{har}}(t)$ denotes the x-component of a branch of an uncoupled linear oscillator, i.e., $x_1(t) = \psi_{\mathrm{har}}(t) = \cos(t)$. As we remarked before, $\psi' \sim 0$ corresponds to the switch in the phase definition from one stable branch to the other. We verify that the evaluation of J_1

under given $\mathbf{x}(t)$ is

(3.9)
$$\frac{d}{dt}J_1 = \nabla(J_1)\cdot\dot{\mathbf{x}} = \begin{pmatrix} -1/(\omega y_1) \\ 0 \\ 1/(-1-x_2+8y_2^3)) \\ 0 \end{pmatrix} \cdot \begin{pmatrix} \omega y_1 + \epsilon g_1(\mathbf{x}) \\ -\omega x_1 \\ -1-x_2+8y_2^3+\epsilon g_2(\mathbf{x}) \\ \epsilon^{-1}(-x_2+y_2-y_2^2) \end{pmatrix}$$
$$= \epsilon\left[\frac{g_2(\mathbf{x})}{-1-x_2+8y_2^3} - \frac{g_1(\mathbf{x})}{\omega y_1}\right].$$

More generally, for a system of the form

(3.10)
$$\begin{cases} \dot{x}_1 &= f_1(x_1,y_1)+\epsilon g_1(\mathbf{x}) \\ \dot{y}_1 &= f_2(x_1,y_1) \\ \dot{x}_2 &= f_3(x_2,y_2)+\epsilon g_2(\mathbf{x}) \\ \dot{y}_2 &= f_4(x_2,y_2), \end{cases}$$

where, for $\epsilon = 0$, (x_1, y_1) and (x_2, y_2) are oscillators of the types described above, the time evolution of the (slow) relative phase is given by

(3.11)
$$\frac{d}{dt}J_1 = \nabla(J_1)\cdot\dot{\mathbf{x}} = \epsilon\left[\frac{g_2(\mathbf{x})}{f_3(x_2,y_2)} - \frac{g_1(\mathbf{x})}{f_1(x_1,y_1)}\right].$$

Setting up the algorithm one needs to be careful near transitions between different branches. Recall that J_1 is the difference between phases whose time derivatives are $1 + O(\epsilon)$. Therefore, one can eliminate the singularities that occur when f_1 or f_3 vanishes by employing a cutoff.

A second problem happens when $f_1(\mathbf{x}_{\rm mid})$ or $f_3(\mathbf{x}_{\rm mid})$ vanish since the left hand side of (3.7) vanish as well. This can be easily avoided by extending the micro simulation by a single extra period, i.e., we integrate the system in a time segment $\tilde{\mathcal{I}} = [t_k, t+k+\eta+T_0]$. We then choose $\mathcal{I}$ as a segment of length η within $\tilde{\mathcal{I}}$ with a convenient mid-point. Since T_0 is of order one, the additional cost (per Macro step) is independent of ϵ.

4. Numerical Examples

In this section we describe a few examples of coupling between different oscillators.

4.1. **Van der Pol-harmonic coupling.**

Consider the following system

(4.1)
$$\begin{cases} \dot{x}_1 &= y_1+\epsilon A x_2 \\ \dot{y}_1 &= -x_1+\epsilon(1-x_1^2)y_1 \\ \dot{x}_2 &= (1+\epsilon\omega)y_2 \\ \dot{y}_2 &= -(1+\epsilon\omega)x_2, \end{cases}$$

with initial conditions $x_1 = y_1 = x_2 = 1$ and $y_2 = 0$. The parameter A is a coupling constant and is independent of ϵ. With $A = 0$, (x_1, y_1) is a Van der Pol oscillator

(1.1) with $\nu = \epsilon$ and (x_2, y_2) is a harmonic oscillator with a frequency $(1+\epsilon\omega)/2\pi$. Hence, the difference between the frequencies of the two oscillators is of order ϵ. For $A \neq 0$ the two oscillators are coupled weakly.

Following the discussion of Section 3, the slow charts for (4.1) includes two amplitudes and a the relative phase, and it spans a three dimensional subspace for each $\mathbf{x}(t)$ away from the turning points. We denote $\xi = (I_1, I_2, J_1)$ with

$$\begin{aligned} I_1 &= I_{\rm vdp}(x_1, y_1) = x_1^2 + y_1^2 \\ I_2 &= I_{\rm har}(x_2, y_2) = x_2^2 + y_2^2 \\ J_1 &= \phi_{\rm har}(x_2, y_2) - \phi_{\rm vdp}(x_1, y_1). \end{aligned} \tag{4.2}$$

Alternatively, since the leading order term in (4.1) is linear, following [1], it is possible to replace J_1 by

$$\xi_3 = x_1 x_2 + y_1 y_2. \tag{4.3}$$

Indeed, $\xi = (I_1, I_2, \xi_3)$ is a slow chart for (4.1).

The algorithm described in Section 2.1 was implemented using the slow chart ξ defined in (4.2) with $\epsilon = 10^{-4}$, $\omega = 10$. Initial conditions are $x_1(0) = y_1(0) = x_2(0) = 1$ and $y_2(0) = 0$. We compare results for $A = 0$ and $A = 10$. Figure 4 depicts the time evolution of the amplitude of the Van der Pol oscillator, $I_1 = x_1^2 + y_1^2$. In order to observe the effect of the relative phase, we plot in Figure 5 the values of x_1 and x_2 during three different runs of the micro-solver. In Figure 5a, $A = 0$ and the two oscillators are decoupled. We see that the two oscillators slowly drift out of phase due to the slightly different frequencies. With $A = 10$ the oscillators are coupled and maintain a constant relative phase. The phenomenon of phase locking, (also called entrainment or synchronization) is well known for linear oscillators [7, 11].

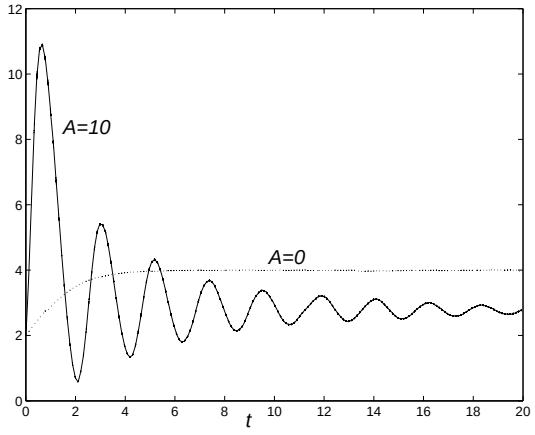

FIGURE 4. The amplitude of the Van der Pol oscillator described by (4.1). $A = 0$: decoupled and $A = 10$: coupled to a harmonic oscillator with a slightly different frequency.

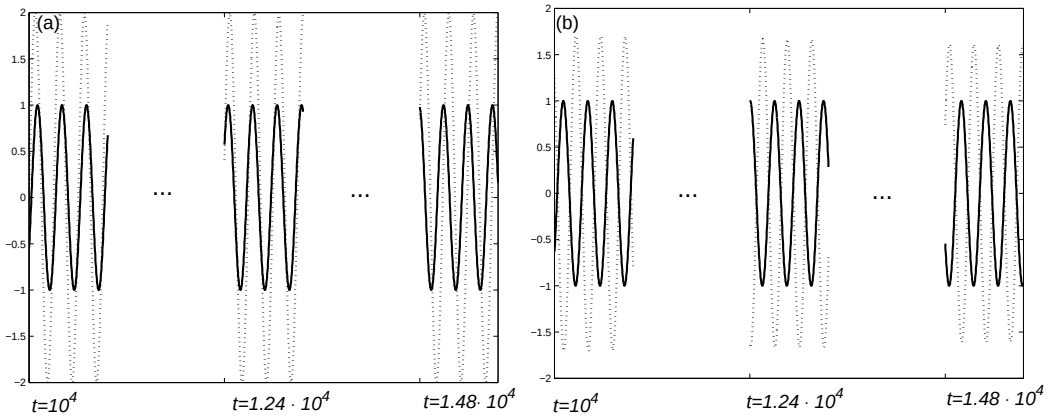

FIGURE 5. The phase of the Van der Pol and harmonic oscillators described by (4.1). (a) $A = 0$: decoupled, and (b) $A = 10$: coupled to a harmonic oscillator with a slightly different frequency. Dotted line: Van der Pol oscillator, solid line: harmonic. The two oscillators are synchronized when coupled.

4.2. **Relaxation-harmonic coupling.** Consider the following system

$$\begin{cases} \dot{x}_1 &= -1 - x_1 + 8y_1^3 + \epsilon A x_2 \\ \dot{y}_1 &= \epsilon^{-1}(-x_1 + y_1 - y_1^3) \\ \dot{x}_2 &= (\omega_0 + \epsilon\omega) y_2 \\ \dot{y}_2 &= -(\omega_0 + \epsilon\omega) x_2, \end{cases} \tag{4.4}$$

where $\omega_0 = 2\pi/T_0$ and T_0 is the period of the decoupled (x_1, y_1) oscillator. Initial conditions are $x_1 = 0$, $y_1 = -1$, and $x_2 = y_2 = 1/\sqrt{2}$. The parameter A is a coupling constant and is independent of ϵ. With $A = 0$, (x_1, y_1) is the relaxation oscillator (3.4) and (x_2, y_2) is a harmonic oscillator with frequency $(\omega_0 + \epsilon\omega)/2\pi$. Hence, the frequencies of the two oscillators are close. For $A \neq 0$ the two oscillators are coupled weakly.

Following the discussion of Section 3 the slow variables for (4.1) can be taken to be the amplitude of the harmonic oscillator and the relative phase, and away from turning points, it spans a two dimensional subspace along the trajectory. Recall that the amplitude of the relaxation oscillator is dissipative. We denote $\xi = (I_1, J_1)$, where

$$\begin{aligned} I_1 &= I_{\rm har}(x_2, y_2) = x_2^2 + y_2^2 \\ J_1 &= \phi_{\rm har}(x_2, y_2) - \phi_{\rm rlx}(x_1, y_1). \end{aligned} \tag{4.5}$$

The algorithm described in Section 2.1 was implemented using the above slow variables with $\epsilon = 10^{-4}$, $\omega = 10$. Time derivatives of J_1 were calculated using (3.9) with a cutoff to exclude points in which either $\dot{x}_1$ or $\dot{x}_2$ vanish. The micro-solver, integrating the full system (4.4) was implemented using a variable step size method in order to speed up integration along the stable branches of the limiting cycle.

Hence, our scheme operates on three time scales: ϵ, 1 and ϵ^{-1}. We compare results for $A = 0$ and $A = 40$. Figure 5 depicts the values of x_1 and x_2 during three different runs of the micro-solver. In Figure 6a, $A = 0$ and the two oscillators are decoupled. We see that the two oscillators slowly drift out of phase due to the slight difference in oscillator frequencies. With $A = 40$ the oscillators are coupled and maintain a constant relative phase. Figure 7 depicts the solution of (4.4) with $\omega_0 = 4\pi/T_0$, i.e, the frequency of the harmonic oscillator is slightly different than twice the frequency of the relaxation oscillator. With $A = 40$ the relaxation oscillator is synchronized with exactly half the frequency of the harmonic one. This phenomenon is referred to 1-2 entrainment or resonance.

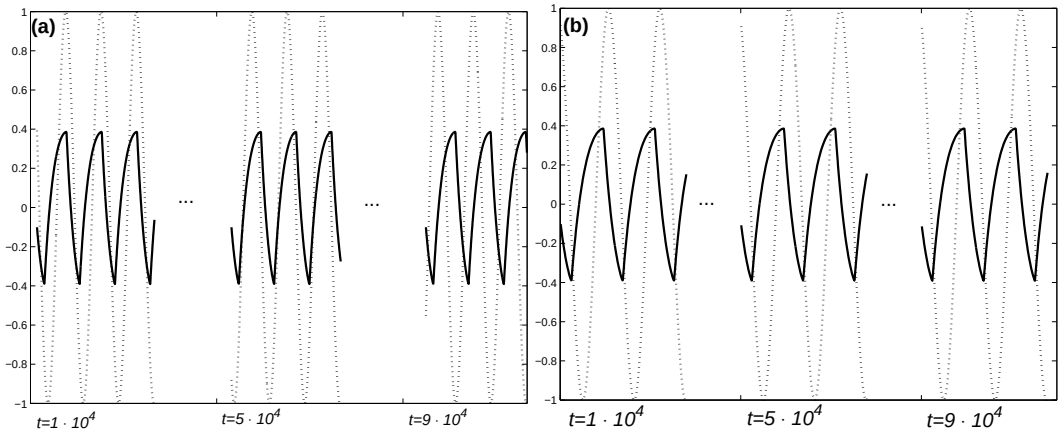

FIGURE 6. The phase of the relaxation and harmonic oscillators described by (4.4). (a) decoupled, $A = 0$, and (b) coupled, $A = 40$, to a harmonic oscillator with a slightly different frequency. Dotted line: harmonic oscillator, solid line: relaxation. The two oscillators are synchronized when coupled.

5. TIME DEPENDENT HARMONIC OSCILLATORS

In this section we apply our method described above to systems of the form

$$\dot{\mathbf{x}} = A(\epsilon t)\mathbf{x} + \epsilon f(\mathbf{x}),\ \mathbf{x}(0) = \mathbf{x}_0, \tag{5.1}$$

where $\mathbf{x} \in \mathbb{R}^{2k}$ and $A(\epsilon t)$ is a smooth $2k \times 2k$ real matrix that is diagonalizable by a smooth similarity transform $P(t)$ and $P(t)^{-}1$ for $t \in \mathcal{I} = [0, \epsilon^{-1}T]$. We assume that the eigenvalues are uniformly bounded away from zero in $\mathcal{I}$ and have non-positive real parts. Without loss of generality we consider the case in which all eigenvalues are purely imaginary. Eigenvalues with negative real part correspond to dissipative variables, which were discussed in Section 2. Finally, we assumed that (5.1) has a unique solution in $\mathcal{I}$.

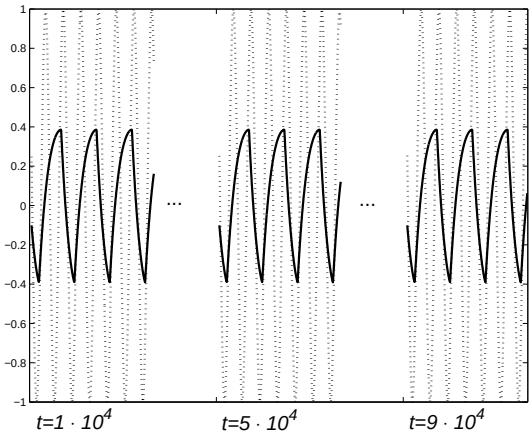

FIGURE 7. Example of 1-2 entrainment between a relaxation oscillator and a harmonic one. Dotted line: harmonic oscillator, solid line: relaxation.

We rewrite (5.1) as

$$\begin{aligned} \dot{\mathbf{x}} &= A(s)\mathbf{x} + \epsilon f(\mathbf{x}), \quad \mathbf{x}(0) = \mathbf{x}_0 \\ \dot{s} &= \epsilon, \qquad\qquad\qquad\quad s(0) = 0, \end{aligned} \tag{5.2}$$

and denote $\mathbf{x} = (x_1, y_1, \ldots, x_k, y_k)$ and $f(\mathbf{x}) = (f_{1,x}, f_{1,y}, \ldots, f_{k,x}, f_{k,y})$. The above assumptions imply that $A(s)$ can be written as $A(s) = P(s)\Lambda(s)P^{-1}(s)$, where $P(s)$ is an invertible matrix with bounded inverse $P^{-1}(s)$ and $\Lambda(s)$ has 2×2 blocks on its diagonal and takes the form

$$\Lambda(s) = \begin{pmatrix} 0 & \lambda_1(s) & & & \\ -\lambda_1(s) & 0 & & & \\ & & \ddots & & \\ & & & 0 & \lambda_k(s) \\ & & & -\lambda_k(s) & 0 \end{pmatrix}. \tag{5.3}$$

By assumption, $\inf_{t\in I} \inf_{i=1\ldots k} |\lambda_i(\epsilon t)| \geq C_0 > 0$. In order to integrate (5.2) using the algorithm described in Section 2 one needs to identify $2k$ slow variables. The variable s is trivially slow. The rest of the slow variables can be classified as k amplitudes of k harmonic oscillators and $k-1$ relative phases. Note that our algorithm makes no explicit use of the decomposition of $A(s)$.

For simplicity, we first suppose that $P(s)$ is the identity matrix for all s. Then, for all $j = 1 \ldots k$, (x_j, y_j) is an harmonic oscillator with amplitude

$$I_j(\mathbf{x}) = x_{2j-1}^2 + x_{2j}^2. \tag{5.4}$$

It is easily verified that $\dot{I}_j(\mathbf{x}) = 2\epsilon(x_j f_{k,j} + y_j f_{j,y})$ and are slow with respect to (5.2). At $\epsilon = 0$, the oscillators are decoupled and the amplitudes are constants. Let $\mathbf{X}(t) = (X_1(t), Y_1(t), \ldots, X_k(t), Y_k(t)$ denote the solution of (5.2) with $\epsilon = 0$.

Also, for $j = 1 \dots k-1$ let $J_j(\mathbf{x}) = X_1^{-1}(\mathbf{x}) - X_j^{-1}(\mathbf{x})$, where $X_j^{-1} : \mathbb{R} \mapsto \mathbb{R}$ denotes the inverse function of $X_j(t)$ (which exists locally). We have that

$$\begin{aligned} \frac{d}{dt} J_j(\mathbf{x}(t)) &= \left[\nabla_{\mathbf{x}} X_1^{-1}(\mathbf{x})\right]_{\mathbf{x}=\mathbf{x}(t)} \cdot \dot{\mathbf{x}}(t) - \left[\nabla_{\mathbf{x}} X_j^{-1}(\mathbf{x})\right]_{\mathbf{x}=\mathbf{x}(t)} \cdot \dot{\mathbf{x}}(t) \\ &= \frac{\dot{x}_1(t)}{\dot{X}_1(t)} - \frac{\dot{x}_j(t)}{\dot{X}_j(t)} = \frac{y_1(t) + \epsilon \partial_x f_1}{Y_1(t)} - \frac{y_j(t) + \epsilon \partial_x f_j}{Y_j(t)} \\ &= \epsilon \left[\frac{\partial_x f_1}{Y_1(t)} - \frac{\partial_x f_j}{Y_j(t)} \right] + \frac{y_1(t) - Y_1(t)}{Y_1(t)} - \frac{y_j(t) - Y_j(t)}{Y_j(t)}. \end{aligned} \tag{5.5}$$

From the theory of averaging [1, 12], we have that the difference between y_j and Y_j is of the order of ϵ, i.e.

$$\sup_{t \in I} |y_i(j) - Y_j(t)| \leq C\epsilon, \tag{5.6}$$

for all $j = 1 \dots k$ and some constant $C > 0$ that does not depend on ϵ. We conclude that $J_j(\mathbf{x})$ is slow with respect to (5.2). Summarizing, we have found that $\xi = (I_1, \dots, I_k, J_1, \dots, J_{k-1}, s)$ is a slow chart for (5.2).

Generalization of the analysis above to any invertible and smooth change of basis matrix $P(t)$ is as follows. First, assume that the eigenvalues $\lambda_1(s) \dots \lambda_k(s)$ are distinct for all s. Then, for fixed s, there exist k constant free quadratic polynomials $I_j(\mathbf{x})$, $j = 1 \dots k$ that are slow with respect to to (5.2). Since $A(s)$ is smooth, there exists k variables $I_j(s, \mathbf{x})$ such that $\nabla_{\mathbf{x}} I_j \cdot A\mathbf{x} = 0$ for all $\mathbf{x} \in \mathbb{R}^{2k}$ and $s \in [0, T]$. Due to (5.3), I_j are quadratic polynomials in $\mathbf{x}$ with time dependent coefficients. We approximate the s dependence of I_k by a polynomial of degree m

$$I_j(\mathbf{x}, s) = \sum_{1 \leq |\mathbf{i}| \leq 2} \left(\sum_{l=0}^{m} c_{\mathbf{i},l}^{j} s^l \right) \mathbf{x}^{\mathbf{i}}, \tag{5.7}$$

where we used multi-index notation $\mathbf{i} \in \mathbb{N}^{2k}$ and $\mathbf{x}^{\mathbf{i}} = x_1^{i_1} y_1^{i_2} \dots x_k^{2k-1} y_k^{2k}$. In [1] we describe how to evaluate the coefficient of such multi-index polynomials from their values on a grid.

In order to identify the relative phase among the oscillators we use the following definition. We say that the i'th coordinate (out of $2k$) participates in I_j if $|I_j(\mathbf{e}_i)|$ is larger than some threshold. Here, $\mathbf{e}_i$ denotes the standard basis for $\mathbb{R}^{2k}$. Let the coordinate i_j participate in I_j with $i_1 \neq i_j$. Then, for all $j = 1 \dots k-1$, $J_j(\mathbf{x}) = X_{i_1}^{-1}(\mathbf{x}) - X_{i_j}^{-1}(\mathbf{x})$ is slow with respect to (5.2) . As before, $\xi = (I_1, \dots, I_k, J_1, \dots, J_{k-1}, s)$ is a slow chart for (5.2).

This suggests the following algorithm for integrating (5.2). Notations are the same as in section 2.1

(1) Initial conditions: $\mathbf{x}(0) = \mathbf{x}_0$ and $n = 0$.
(2) micro-simulation: Solve (5.2) in $[t_n - \eta, t_n + \eta]$ with initial conditions $\mathbf{x}(t_n) = \mathbf{x}_n$.
(3) Slow variables:

(a) Find k quadratic slow variables $I_1 \dots I_k$.
(b) Find k distinguished coordinates $i_1 \dots i_k$ that participate in $I_1 \dots I_k$, respectively.
(c) take $\xi = (I_1, \dots, I_k, J_1, \dots, J_{k-1}, s)$.

(4) Averaging: approximate $\dot{\xi}(t_n)$ by $\langle \dot{\xi}(t_n) \rangle_\eta$.
(5) Macro-step (forward Euler example): $\mathbf{x}_{n+1} = \mathbf{x}_{\text{mid}} + H\delta\mathbf{x}$, where $\delta\mathbf{x}$ is the least squares solution to the linear system

$$\delta\mathbf{x} \cdot \nabla\xi_i(\mathbf{x}_{\text{mid}}) = F_i(\xi(\mathbf{x}_{\text{mid}})) = \langle \dot{\xi}_i \rangle_\eta,$$

for all $i = 1 \dots 2k$.
(6) $n = n + 1$. repeat steps (2) through (5) to time $\epsilon^{-1}T$.

Suppose that, for some $s_i = \epsilon t_i$ we have that $\lambda_1(s_i) = \lambda_2(s_i)$, and different otherwise. In this case, we have a degeneracy of the slow subspace along the trajectory. As explained in [1], in addition to I_1 and I_2, the relative phase between the first two oscillators can also be described by two equivalent quadratic polynomials. For example, for $k = 2$ if $P(s_i)$ is the identity matrix than both $K_1(\mathbf{x}) = x_1x_2 + y_1y_2$ and $K_1(\mathbf{x}) = x_1y_2 - x_2y_1$ are slow. In other words, at the resonance $\lambda_1 = \lambda_2$, there are four linearly independent quadratic slow variables rather than two. However, I_1, I_2, J_1, K_1 and K_2 are not functionally independent. For this reason one needs to eliminate K_1 and K_2 and keep the slow variables that correspond to amplitudes, so that the same structure of the slow chart $\xi = (I_1, I_2, J_1)$ is kept throughout the algorithm. The relative phase J_1 is calculated in the same way as away from the resonance, by parametrization with respect to time along the branches of the trajectory. In order to eliminate the two extra quadratic variables we note that the eigenvalues only coincide at $s = s_i$. Finding the coefficients of (5.7) requires solving a least squares problem on a grid. Using a large, $O(\epsilon^{-1})$, grid spacing in the temporal coordinate s will greatly reduce the fit of the phase-related polynomials.

As an example, we applied the above algorithm to a system of two oscillators ($k = 2$) with $\lambda_1(s) = 0.8$, $\lambda_2(s) = 0.5 + s$, $\epsilon = 10^{-4}$ and $I = [0, \epsilon^{-1}]$. Hence, the system passes through a $1 - 1$ resonance at $s = 0.3$ ($t = 3000$). Also,

$$P(s) = \begin{pmatrix} 1 & 1 & s & -1 \\ -1 & 2 & 2 & -s \\ 0 & 2s & 1 & 1 \\ s & -2 & -s/2 & 0 \end{pmatrix}, \; f(\mathbf{x}) = \begin{pmatrix} y_1 \\ 0 \\ -y_2 \\ 0 \end{pmatrix}. \tag{5.8}$$

Since only linear combinations of slow variables, rather than the detected ones, are defined uniquely, it is difficult to compare the time evolution of the slow variables themselves between different simulation methods. Instead, Figure 8 depicts the time evolution of two local averages $\langle x_1^2 \rangle_\eta$ and $\langle y_2^2 \rangle_\eta$, which are also slow for sufficiently large η [1]. Simulation parameters are $H = 0.1\epsilon^{-1}$, $\eta = 70$, $m = 2$, $a = 1$ and $b = 0.05\epsilon^{-1}$. Both Macro and micro solvers use an fourth order Runge-Kutta scheme. We see that around the 1-1 resonance x^2 ceases to be a fast variable and the related local time averages develops minor oscillations. For this reason it takes

larger values of η to smooth out oscillations. On the other hand, slow variables are consistently slow throughout the integration even around resonances.

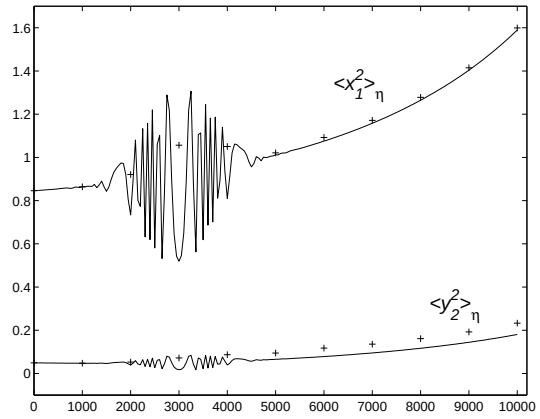

FIGURE 8. Local time averages for a system of two time dependent linear oscillators. Solid line - fourth order Runge-Kutta method and plus symbols - HMM. At $t = 3000$ the two oscillators are in resonance and the local averages are not slow.

Finally, we would like to remark on the significance of the assumption that $A(s)$ defined in (5.1 is smoothly diagonalizable for all s. This condition is important in order to guaranty that the dynamics of (5.1) can b described by slow charts that consists of $2k$ variables plus a single fast harmonic oscillator. However, this assumption fails in several interesting situations. In this case the method described above fails since there may not be a uniform separation between a slow and fast time scales. The standard way for integrating over such turning points efficiently is by using variable size steps [10, 13] .

6. CONCLUSION

In [1] we propose a general approach for decomposing a vector field into its fast and slow constituents using polynomials. The decomposition is used in an algorithm that efficiently integrates the slow parts of the dynamics without fully resolving the fast parts. In this paper we further develop this idea and extend it to fully nonlinear oscillators. This is different from oscillations in systems whose Jacobian have large purely imaginary eigenvalues. In other words, the oscillators cannot be locally approximated as harmonic. We study how to compute the correct coupling of such oscillators in the weak coupling limit. We present several examples in which the oscillators, when uncoupled, are either constrained to a periodic solution or are attracted rapidly to an invariant manifold.

The slow variables are classified as amplitudes and relative phases, in analogy to corresponding variables for harmonic oscillators. The notion of relative phase is defined by parametrizing the stable branches of the invariant manifold according

to time. Some specific knowledge of the orbits of uncoupled oscillators is needed. Following the HMM framework, the time evolution of the slow variables in the coupled system is computed using on the fly short-time simulations of the full system. Thus, we are able to compute the slow behavior of the system using large time steps.

Finally, we see that a similar approach provides an efficient numerical algorithm for a class of weakly coupled harmonic oscillators with time dependent, slowly varying frequencies. If two or more eigenvalues cross, then the system is in resonance and may exhibit non-trivial slow behavior. None the less, the algorithm proposed is consistent as long as the leading part of the dynamics is diagonalizable.

ACKNOWLEDGMENTS

Support from NSF through Grant DMS-0714612 is gratefully acknowledged. Tsai's research is partially supported by an Alfred P. Sloan Fellowship. Tsai and Engquist thank the Isaac Newton Institute for Mathematical Sciences for hosting parts of this research. Tsai also thanks the National Center for Theoretical Sciences at Taipei.

REFERENCES

[1] G. Ariel, B. Engquist, and R. Tsai. A multiscale method for highly oscillatory ordinary differential equations with resonance. *Math. Comp.* submitted. A preprint is available as a UCLA CAM report.

[2] G. Dahlquist, L. Edsberg, G. Skollermo, and G. Soderlind. Are the numerical methods and software satisfactory for chemical kinetics? In *Numerical Integration of Differential Equations and Large Linear Systems*, volume 968 of *Lecture Notes in Math.*, pages 149–164. Springer-Verlag, 1982.

[3] W. E. Analysis of the heterogeneous multiscale method for ordinary differential equations. *Commun. Math. Sci.*, 1(3):423–436, 2003.

[4] W. E and B. Engquist. The heterogeneous multiscale methods. *Commun. Math. Sci.*, 1(1):87–132, 2003.

[5] B. Engquist and Y.-H. Tsai. Heterogeneous multiscale methods for stiff ordinary differential equations. *Math. Comp.*, 74(252):1707–1742, 2003.

[6] J. Grasman. *Asymptotic methods for relaxation oscillations and applications*, volume 63 of *Applied Mathematical Sciences*. Springer-Verlag, 1987.

[7] J. Guckenheimer and P. Holmes. *Nonliner oscillations, dynamical systems and bifurcations of vector fields*, volume 42 of *Applied Mathematical Sciences*. Springer-Verlag, 1990.

[8] E. Hairer, C. Lubich, and G. Wanner. *Geometric numerical integration*, volume 31 of *Springer Series in Computational Mathematics*. Springer-Verlag, Berlin, 2002. Structure-preserving algorithms for ordinary differential equations.

[9] M. Hochbruck, C. Lubich, and H. Selhofer. Exponential integrators for large systems of differential equations. *SIAM J. Sci. Comp.*, 19:1552–1574, 1998.

[10] H.-O. Kreiss. Difference methods for stiff ordinary differential equations. *SIAM J. Numer. Anal.*, 15(1):21–58, 1978.

[11] A. Pikovsky, M. Rosenblum, and J. Kurths. Phase synchronization in regular and chaotic systems. *Int. J. Bifurcation and Chaos*, 10(10):2291–2305, 2000.

[12] J. A. Sanders and F. Verhulst. *Averaging Methods in Nonlinear Dynamical Systems*, volume 59 of *Applied Mathematical Sciences*. Springer-Verlag, New York, Berlin, Heidelberg, Tokyo, 1985.
[13] R. E. Scheid. Difference methods for problems with different time scales. *Math. Comp.*, 44(169):81–92, 1985.
[14] B. Van der Pol. On relaxation oscillations. *Phil. Mag. 2*, 2:978–992, 1926.

DEPARTMENT OF MATHEMATICS, THE UNIVERSITY OF TEXAS AT AUSTIN, AUSTIN, TX, 78712, USA

E-mail address: ariel@math.utexas.edu

E-mail address: engquist@math.utexas.edu

E-mail address: ytsai@math.utexas.edu